Vol.2012-MPS-88 No.10
2012/5/17

Estimating Distribution of Dendritic Membrane Resistance Using Markov Random Field

Jun Kitazono ,[†1] Toshiaki Omori ,[†2] Toru Aonishi [†3] and Masato Okada[†1,†4]

With developments in optical imaging over the past decade, statistical methods for estimating dendritic membrane resistance from observed noisy signals have been proposed. In most of previous studies, membrane resistance over a dendritic tree was assumed to be constant, or membrane resistance at a point rather than that distributed over a dendrite was investigated. Membrane resistance, however, is actually non-uniformly distributed. Although in a previous study a method was proposed in which a specific non-homogeneous distribution form was assumed, it is applicable only when the appropriate distribution form is known. We propose a statistical method, that does not assume a particular distribution form of membrane resistance, for estimating membrane resistance distribution from observed membrane potentials. We use the Markov random field (MRF) as a prior of the membrane-resistance distribution. In the MRF, any specific distribution form of membrane resistance is not assumed, but only spatial smoothness of membrane resistance is assumed. We apply our method to synthetic data to evaluate its efficacy, and show that even when we do not know the appropriate distribution form, our method can accurately estimate the membrane-resistance distribution.

1. Introduction

Information processing in neural systems is suggested to be dependent on how the membrane properties are distributed over dendritic trees[1)–7)]. In hippocampal CA1 pyramidal neuron dendrites, for example, the membrane resistance is non-uniformly distributed. A recent computational study showed that this non-uniformity improves the efficiency of information propagation from the distal to proximal parts[6)].

With developments in optical imaging over the past decade, several statistical methods for estimating membrane properties, especially membrane resistance, from fluorescence intensity have been proposed[4),5),7)–9)]. Optical imaging, however, has a low signal-to-noise ratio[10)–17)], so accurately estimating membrane resistance over a dendritic tree is challenging. In previous studies, membrane resistance over a dendritic tree was assumed to be constant, or membrane resistance at a point rather than that distributed over a dendrite was investigated. We previously proposed a method in which a specific distribution form was assumed[4),5),7)]. Although this method can accurately estimate membrane resistance over a dendrite, it is applicable only when we know the appropriate distribution form. Thus, developing methods for estimating membrane resistance over a dendrite remains a challenge.

For this study, we propose a statistical method, which does not assume a particular distribution form of membrane resistance, for estimating membrane resistance distributions from observed noisy signals. For this purpose, we use the Markov random field (MRF)[18),19)] as a prior of the membrane-resistance distribution. In the MRF, any specific distribution form of membrane resistance is not assumed, but only spatial smoothness of membrane resistance is assumed. This smoothness prior expresses a physiological premise that spatially adjacent membrane resistances take similar values. Additionally, the dynamics of membrane potential corresponding to a state in dendritic systems is expressed using the cable equation[20),21)], and the observation process is expressed using a Gaussian process. We estimate parameters, namely, membrane-resistance distribution by using the expectation-maximization (EM) algorithm[22)]. We applied our method to synthetic data to evaluate its efficacy, and show that even when we do not know the appropriate distribution form, our method can accurately estimate the membrane-resistance distribution.

2. Formulation

In this section, we describe the three probabilistic models that we use in our

†1 Graduate School of Frontier Sciences, The University of Tokyo
†2 Graduate School of Engineering, Kobe University
†3 Interdisciplinary Graduate School of Science and Engineering, Tokyo Institute of Technology
†4 RIKEN Brain Science Institute

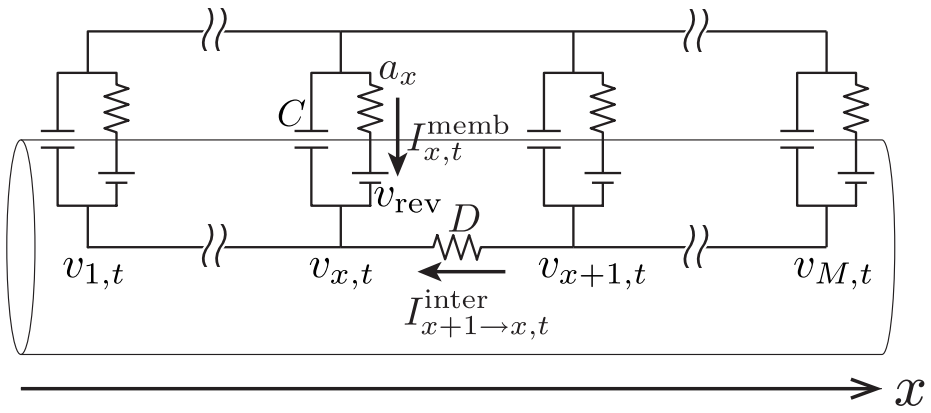

Fig. 1 Schematic of compartment model. Compartment model is a spatially discrete approximation of the cable equation. Membrane current $I^{\text{memb}}_{x,t}$ and current along dendrite $I^{\text{inter}}_{x+1\to x,t}$ are given as $-a_x(v_{x,t}-v_{\text{rev}})$ and $D(v_{x+1,t}-v_{x,t})$, respectively. $v(x,t)$ is membrane potential at position x at time t, which expresses electrical state of dendrite. a_x, D, and C are membrane conductance at position x, intercompartmental conductance, and membrane capacitance, respectively. These three parameters define electrical property of dendrite. Stationary distribution of this compartment model is expressed as a Gaussian distribution. In our method, distribution of membrane conductance a_x is estimated using Markov Random Field (MRF). Unlike the previous studies, in our method any specific distribution form is not assumed but only spatial smoothness of the membrane conductance a_x is assumed by using MRF.

method. Using these probabilistic models enables us to estimate the membrane-resistance distribution of dendrite from observed noisy membrane potential. In subsection 2.1, we describe the cable equation[20], which expresses the dynamics of the dendritic membrane potential, and its spatially discrete approximation, the compartment model[21]. We then derive the stationary distribution of the compartment model. In subsection 2.2, we explain the smoothness prior, based on the MRF[18),19)], of the membrane resistance. The smoothness prior assumes that spatially adjacent membrane resistances take similar values, to accurately estimate membrane resistance distribution over a dendrite, even when observation process is noisy. In subsection 2.3, we describe the observation model, which expresses the noisy observation of membrane potential.

2.1 Cable equation and stationary distribution for compartment model

In the cable equation[20], the dynamics of the membrane potential is given as

$$C\frac{\partial v(x,t)}{\partial t} = -a_x\left(v(x,t)-v_{\text{rev}}\right) + D\frac{\partial^2 v(x,t)}{\partial x^2} + u(x,t) + \sigma\xi(x,t), \qquad (1)$$

where $v(x,t)$ is the membrane potential at position x at time t. In this paper, we consider a one-dimensional dendrite for the sake of simplicity. The right-hand side of eq. (1) consists of four terms. The first term $-a_x\left(v(x,t)-v_{\text{rev}}\right)$ expresses a passive linear membrane current, where a_x is the membrane conductance (inverse of membrane resistance) at position x and v_{rev} expresses reversal potential. The objective of our study was to estimate membrane conductance a_x from the observed membrane potential. The second term $D\frac{\partial^2 v(x,t)}{\partial x^2}$ expresses a current along the dendrite, where D is the intercompartmental conductance. The third term $u(x,t)$ expresses an external input, and the last term $\sigma\xi(x,t)$ expresses the internal noise of the neuron that is assumed to be white Gaussian with average $\langle\xi(x,t)\rangle = 0$ and correlation function $\langle\xi(x,t)\xi(x',t')\rangle = \delta(x-x')\delta(t-t')$. Parameter C on the left-hand side of eq. (1) is the membrane capacitance. We can assume $C=1$ without loss of generality. Next, we introduce a spatially discrete approximation to the cable equation: the compartment model[21]. A schematic of the compartment model is shown in **Fig. 1**. In this model, a dendrite is segmented into small compartments and the cable equation (1) is approximated as follows:

$$v_{x,t+1}-v_{x,t} = \Delta t\left\{-a_x(v_{x,t}-v_{\text{rev}}) + D(v_{x-1,t}-2v_{x,t}+v_{x+1,t}) + u_{x,t}\right\} + \sqrt{\Delta t}\epsilon_{x,t}, \qquad (2)$$

where $v_{x,t}$, $u_{x,t}$ and $\epsilon_{x,t}$ are the membrane potential, the external input, and the internal noise assumed to be Gaussian with mean 0 and variance σ^2, at compartment x at time t, respectively.

We derive the stationary distribution of eq. (2) for computational simplicity. Let $\tilde{\boldsymbol{v}}_t = \boldsymbol{v}_t - \boldsymbol{v}_{\text{rev}}$ in eq. (2), where $\boldsymbol{v}_t$ and $\boldsymbol{v}_{\text{rev}}$ are M-dimensional column vectors $(v_{1,t},\cdots,v_{M,t})^T$ and $(v_{\text{rev}},\cdots,v_{\text{rev}})^T$, respectively. M is the number of

compartments. We then obtain

$$\tilde{\boldsymbol{v}}_{t+1} = \Phi\tilde{\boldsymbol{v}}_t + \Delta t\left(\boldsymbol{u}_t + \frac{1}{\sqrt{\Delta t}}\boldsymbol{\epsilon}_t\right), \tag{3}$$

$$\Phi = I - \Delta t\Psi, \tag{4}$$

$$\Psi = \begin{pmatrix} a_1 & & \\ & \ddots & \\ & & a_M \end{pmatrix} + D\begin{pmatrix} 1 & -1 & & & \\ -1 & 2 & -1 & & \\ & \ddots & \ddots & \ddots & \\ & & -1 & 2 & -1 \\ & & & -1 & 1 \end{pmatrix}, \tag{5}$$

where $\boldsymbol{u}_t = (u_{1,t}, \cdots, u_{M,t})^T$, $\boldsymbol{\epsilon}_t = (\epsilon_{1,t}, \cdots, \epsilon_{M,t})^T$, and I is the identity matrix. This equation is a first-order autoregressive model with Gaussian noise. If we keep the external input $\boldsymbol{u}_t$ constant ($\boldsymbol{u}_t = \boldsymbol{u}$), the probability density function of the true membrane potential converges to the stationary distribution as $t \to \infty$. Since eq. (3) is a Gaussian process, the stationary distribution is a Gaussian distribution. Therefore, we just need to determine the mean and covariance of the distribution. First, we derive the mean of the stationary distribution $\mathrm{E}[\tilde{\boldsymbol{v}}_\infty]$. By iteratively solving eq. (3), we obtain

$$\tilde{\boldsymbol{v}}_t = \Phi^t\tilde{\boldsymbol{v}}_0 + \Delta t\sum_{s=0}^{t-1}\Phi^s\left(\boldsymbol{u} + \frac{1}{\sqrt{\Delta t}}\boldsymbol{\epsilon}_{t-1-s}\right). \tag{6}$$

Since $\mathrm{E}[\boldsymbol{\epsilon}_t] = \boldsymbol{0}$,

$$\mathrm{E}[\tilde{\boldsymbol{v}}_\infty] = \Delta t\left(I - \Phi\right)^{-1}\boldsymbol{u} \approx \Psi^{-1}\boldsymbol{u}, \tag{7}$$

where we used $\lim_{t\to\infty}\Phi^t = 0$ and $\sum_{s=0}^{\infty}\Phi^s = (I-\Phi)^{-1}$. Next, we derive the covariance matrix $\mathrm{Cov}[\tilde{\boldsymbol{v}}_\infty]$. From eq. (6),

$$\begin{aligned}\mathrm{Cov}[\tilde{\boldsymbol{v}}_t] &= \mathrm{Cov}\left[\Phi^t\tilde{\boldsymbol{v}}_0 + \Delta t\sum_{s=0}^{t-1}\Phi^s\left(\boldsymbol{u} + \frac{1}{\sqrt{\Delta t}}\boldsymbol{\epsilon}_{t-1-s}\right)\right] \\ &= \Delta t\sigma^2\sum_{s=0}^{t-1}\Phi^{2s}.\end{aligned} \tag{8}$$

By taking the limit $t \to \infty$,

$$\mathrm{Cov}[\tilde{\boldsymbol{v}}_\infty] = \Delta t\sigma^2\left(I - \Phi^2\right)^{-1} \approx \frac{\sigma^2}{2}\Psi^{-1}. \tag{9}$$

Thus, the stationary distribution is given as a Gaussian distribution:

$$p\left(\boldsymbol{v}|\boldsymbol{a}\right) = \mathcal{N}\left(\boldsymbol{v}\middle|\boldsymbol{v}_{\mathrm{rev}} + \Psi^{-1}\boldsymbol{u}, \frac{\sigma^2}{2}\Psi^{-1}\right). \tag{10}$$

We omit the subscript ∞ for the sake of notational simplicity. We can rewrite eq. (10) using an energy function $E(\boldsymbol{v}|\boldsymbol{a})$:

$$p(\boldsymbol{v}|\boldsymbol{a}) = \frac{1}{Z(\boldsymbol{a})}\exp\left(-\frac{1}{\sigma^2}E(\boldsymbol{v}|\boldsymbol{a})\right), \tag{11}$$

$$E(\boldsymbol{v}|\boldsymbol{a}) = \sum_{x=1}^{M}a_x(v_x - \bar{v}_x)^2 + D\sum_{x=1}^{M-1}(v_{x+1} - v_x)^2, \tag{12}$$

$$Z(\boldsymbol{a}) = (\pi\sigma^2)^{\frac{M}{2}}|\Psi|^{-\frac{1}{2}}, \tag{13}$$

where $\bar{v}_x$ is the x-th element of $\boldsymbol{v}_{\mathrm{rev}} + \Psi^{-1}\boldsymbol{u}$.

2.2 Prior distribution of membrane conductance

In this subsection, we introduce the smoothness prior, based on the MRF[18),19)], of the membrane conductance. The MRF is represented by a probability density function:

$$p(\boldsymbol{a}) \propto \exp(-E(\boldsymbol{a})), \tag{14}$$

$$E(\boldsymbol{a}) = \lambda\sum_{x=1}^{M-1}(a_{x+1} - a_x)^2, \tag{15}$$

$$a_x \in [0, \infty). \tag{16}$$

This equation expresses a physiological premise that membrane conductances of nearby compartments take similar values. The probability $p(\boldsymbol{a})$ increases if nearby membrane conductances take similar values and decreases if they take dissimilar ones. As mentioned above, the objective of our study was to estimate the spatial distribution of a_x over the dendrite. Accurate estimation of the distribution has been difficult because the signal-to-noise ratio of membrane potential imaging is low. We use the MRF as a prior distribution of membrane conductance, to accurately estimate the distribution even when observation process is noisy, without assuming a membrane-conductance distribution form.

2.3 Observation model

We introduce the observation model, a Gaussian process, which expresses the noisy observation of membrane potential. Let $\boldsymbol{y}_t = (y_{1,t}, \cdots, y_{M,t})^T$ be the observed membrane potential at time t. Then, the observation model is given as

$$p(\boldsymbol{y}_t|\boldsymbol{v}_t) = \frac{1}{(2\pi\eta^2)^{\frac{M}{2}}}\exp\left(-\frac{1}{2\eta^2}E(\boldsymbol{y}_t|\boldsymbol{v}_t)\right), \tag{17}$$

$$E(\boldsymbol{y}_t|\boldsymbol{v}_t) = \sum_{x=1}^{M}(y_{x,t} - v_{x,t})^2. \tag{18}$$

This equation expresses that the observed membrane potential $y_{x,t}$ is the sum of the true membrane potential $v_{x,t}$ and Gaussian noise with variance η^2.

3. Estimation

In this section, we illustrate the estimation method. By using the models eq. (11)–(18) described above, we estimate membrane conductance a_x and potential v_x from observed noisy data y_x. We derive the estimation method based on the EM algorithm[22]. The EM algorithm is a standard method for estimating parameters in statistical models based on the maximum liklihood or the maximum a posteriori principles.

The EM algorithm iterates over two steps, expectation (E-step) and maximization (M-step). In the E-step, we obtain the expectation value of the membrane potential $\boldsymbol{v}$, and in the M-step, we obtain the estimates of the membrane conductance $\boldsymbol{a}$. Let $\boldsymbol{Y} = \{\boldsymbol{y}_1, \ldots, \boldsymbol{y}_N\}$ denote a set of observed membrane potentials and $\boldsymbol{V} = \{\boldsymbol{v}_1, \ldots, \boldsymbol{v}_N\}$ denote a set of corresponding true membrane potentials. Then, the two steps are given as follows:

E-step Based on the current estimate of the parameter $\boldsymbol{a}_{\rm old}$, the conditional distribution of the latent variables $p(\boldsymbol{V}|\boldsymbol{Y}, \boldsymbol{a}_{\rm old})$ is calculated. Then the expected values of $\boldsymbol{V}$, and the expected complete-data loglikelihood $\mathcal{Q}(\boldsymbol{a}, \boldsymbol{a}_{\rm old}) = \langle \log p(\boldsymbol{Y}, \boldsymbol{V}|\boldsymbol{a}) \rangle_{p(\boldsymbol{V}|\boldsymbol{Y}, \boldsymbol{a}_{\rm old})}$ are computed.

$$\begin{aligned}\mathcal{Q}(\boldsymbol{a}, \boldsymbol{a}_{\rm old}) =& \frac{N}{2} \log |\Psi| - \frac{1}{\sigma^2} \sum_i^N \left\{ {\rm Tr}(\Psi(\Sigma + \boldsymbol{v}_{\rm rev} \boldsymbol{v}_{\rm rev}^T)) \right. \\ & \left. + \boldsymbol{m}_i^{\rm T} \Psi \boldsymbol{m}_i - 2 v_{\rm rev} \boldsymbol{m}_i^{\rm T} \boldsymbol{a} + \boldsymbol{u}^{\rm T} \Psi^{-1} \boldsymbol{u} \right\} + {\rm const.},\end{aligned} \tag{19}$$

where $\boldsymbol{m}_i$, Σ are the mean and the covariance of the Gaussian distribution $p(\boldsymbol{v}_i|\boldsymbol{y}_i, \boldsymbol{a}_{\rm old})$.

M-step A new estimation value of the parameter $\boldsymbol{a}_{\rm new}$ is inferred, which maximizes the sum of $\mathcal{Q}(\boldsymbol{a}, \boldsymbol{a}_{\rm old})$ and $\log p(\boldsymbol{a})$:

$$\boldsymbol{a}_{\rm new} = \underset{\boldsymbol{a}}{\rm argmax} \left\{ \mathcal{Q}(\boldsymbol{a}, \boldsymbol{a}_{\rm old}) + \log p(\boldsymbol{a}) \right\}. \tag{20}$$

Starting with the initial setting $\boldsymbol{a}_{\rm old} = \boldsymbol{a}_0$, these two steps are repeated until convergence.

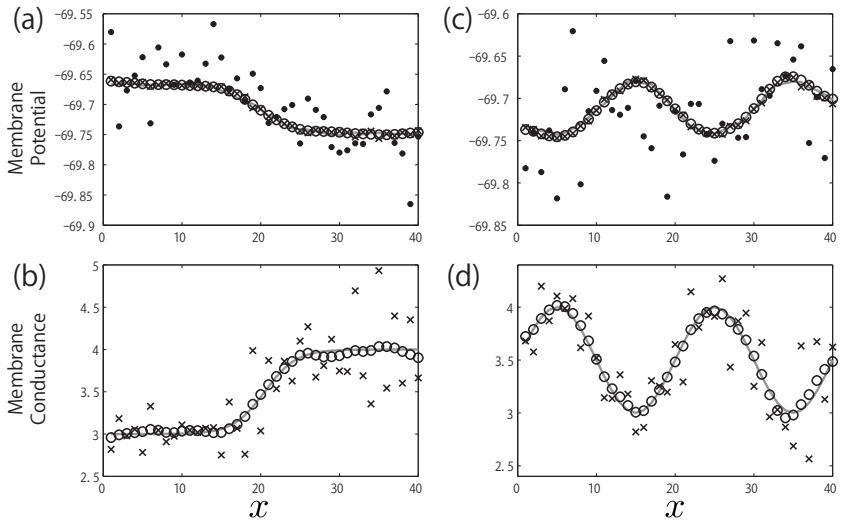

Fig. 2 Estimating parameters for sigmoidal distribution ((a), (b)) and sinusoidal distribution ((c), (d)). Top panels show membrane potential. Sample of observed membrane potential out of N samples is plotted as black circles. Corresponding true membrane potential, estimate using MRF, and estimate without MRF are plotted as gray line, open circles (○), and crosses (×), respectively. Bottom panels show membrane conductance. True membrane conductance, estimate using MRF, and estimate without MRF are plotted as gray line, open circles (○), and crosses (×), respectively.

4. Results

We present results of applying our method to synthetic data. The synthetic data were generated as follows. First, true membrane potentials were generated from the compartment model, eq. (2). Observed membrane potentials $\boldsymbol{Y}$ were then generated from the observation model, eq. (17). We estimated membrane conductance $\boldsymbol{a}$ and membrane potentials $\boldsymbol{V}$ from observed membrane potential $\boldsymbol{Y}$ generated as above. We compared our method to that without the MRF, in which $p(\boldsymbol{a})$ is a uniform distribution in stead of eq. (14). We set $D = 10$, $v_{\rm rev} = -70$, $\sigma = 0.01$, $\Delta t = 0.01$, $\eta = 0.05$, and $\lambda = 100$. The number of samples N was 200.

4.1 Sigmoidal distribution

First, we present the results of applying the methods to the case where membrane conductance distribution is sigmoidal, plotted as a gray line in **Fig. 2**(b). In hippocampal CA1 pyramidal neuron dendrite, sigmoidal membrane-conductance distribution is observed[4),5)]. A sample of observed membrane potential out of N samples is plotted as black circles in Fig. 2(a). The corresponding true membrane potential, estimate using the MRF, and estimate without the MRF are plotted as gray line, open circles (○), and crosses (×), respectively. we can see that the open circles (○) and crosses (×) are almost on the gray line, that is, the estimates of membrane potential agree well with the true membrane potential. The estimates of membrane conductance are plotted in Fig. 2(b). Although our method did not assume that distribution form of membrane conductance is sigmoidal, estimated membrane conductance (○) agrees well with the true membrane conductance. In contrast, the estimate without MRF (×) is less accurate.

4.2 Sinusoidal distribution

Second, we present results of applying the methods to the case where membrane conductance distribution is sinusoidal, to show that out method is applicable not only to the sigmoidal case. As is in the above case, observed membrane potential is plotted as black circles in Fig. 2(c). The true membrane potential, the estimate using the MRF, and the estimate without the MRF are plotted as gray line, open circles (○), and crosses (×), respectively. The membrane potential is plotted in Fig. 2(a). We can see that the open circles (○) and crosses (×) are almost on the gray line, that is, the estimates of membrane potential agree well with the true membrane potential. The estimates of membrane conductance is plotted in Fig. 2(d). The estimate using the MRF (○) agree well with the true membrane conductance, while the estimate without the MRF (×) deviates due to noise.

As presented above, in both sigmoidal and sinusoidal distribution cases, the membrane conductances estimated using the MRF agree well with true membrane conductances, while those estimated without the MRF deviate from the true membrane conductances. Thus, our method, in which the MRF is used as a smoothness prior, enables us to estimate the membrane-resistance distribution accurately even when the appropriate distribution form is unknown.

5. Summary

We proposed a method for estimating the distribution of membrane resistance. The dynamics of the membrane potential are expressed using the compartment model and the observation process was modeled as a Gaussian process. Membrane resistance was estimated using the EM algorithm.

Unlike the previous studies, in which specific distribtion forms of membrane resistance are assumed, in our method any specific distribution form is not assumed but only spatial smoothness of the membrane resistance is assumed by using MRF. We showed using synthetic data that our method can be applied when the appropriate distribution form is unknown.

The stationary distribution of the compartment model is used for computational simplicity. Transient dynamics can be used for estimation by applying Kalman filter to the compartmnet model. We targeted voltage-independent resistance. Our framework using MRF as a prior of membrane resistance distribution can also be applicable to voltage-dependent resistance. This is a subject for further study.

Acknowledgments This work was partially supported by Grant-in-Aid for JSPS Fellows [10J06155(J.K.)], Grant-in-Aids for Scientific Research on Innovative Areas "The study on the neural dynamics for understanding communication in terms of complex hetero systems (Project No. 4103)" [No. 22120506(T.O.)] and "Face perception and recognition: Multidisciplinary approaching to understanding face processing mechanism (Project No. 4002)" [No. 23119708(M.O.)], Grants-in-Aid for Scientific Research (C) [Nos. 20509001(T.O), 23123456(T.A.)], Grant-in-Aid for Scientific Research (A) [No. 20240020(M.O.)] and Grant-in-Aid for Challenging Exploratory Research [No. 22650041(M.O.)] from the MEXT of Japan.

References

1) Johnston, D., Magee, J.C., Colbert, C.M., and Christie, B.R.: Active properties of neuronal dendrites, *Ann. Rev. Neurosci.*, Vol.19, pp.165–186 (1994).
2) Safronov, B.V.: Spatial distribution of Na and K channels in spinal dorsal horn neurones: role of the soma, axon and dendrites in spike generation, *Prog. Neurobiol.*, Vol.60, pp.217–241 (1999).

3) Shepherd, G.M.: *The Synaptic Organization of the Brain*, Oxford University Press, USA, 5th edition (2003).
4) Omori, T., Aonishi, T., Miyakawa, H., Inoue, M., and Okada, M.: Estimated Distribution of Specific Membrane Resistance in Hippocampal CA1 Pyramidal Neuron, *Brain Res.*, Vol.1125 pp.199–208 (2006).
5) Omori, T., Aonishi, T., Miyakawa, H., Inoue, M., and Okada, M.: Steep Decrease in the Specific Membrane Resistance in the Apical Dendrites of Hippocampal CA1 Pyramidal Neurons, *Neurosci. Res.*, Vol.64, pp.83–95 (2009).
6) Omori, T. and Okada, M.: Mathematical Models of Hippocampal System, *Clinical Neuroscience*, Vol.29, No.2, pp.162–166 (2011). (in Japanese).
7) Omori, T., Aonishi, T., and Okada, M.: Statistical Estimation of Non-Uniform Distribution of Dendritic Membrane Properties, to be published in *Advances in Cognitive Neurodynamics (III)*.
8) Huys, Q.J.M. and Paninski, L.: Smoothing of, and Parameter Estimation from, Noisy Biophysical Recordings, *PLoS Comput. Biol.*, Vol.5, e1000379 (2009).
9) Paninski, L.: Fast Kalman filtering on quasilinear dendritic trees, *J. Comput. Neurosci.*, Vol.28, pp.211–228 (2010).
10) Djurisic, M., Antic, S., Chen, W.R., and Zecevic, D.: Voltage imaging from dendrites of mitral cells: EPSP attenuation and spike trigger zones, *J. Neurosci*, Vol.24, pp.6703–6714 (2004).
11) Sacconi, L., Dombeck, D.A., and Webb, W.W.: Overcoming photodamage in second-harmonic generation microscopy: Real-time optical recording of neuronal action potentials, *Proc. Natl. Acad. Sci. USA*, Vol.103, pp.3124–3129 (2006).
12) Araya, R., Eisenthal, K.B., and Yuste, R.: Dendritic spines linearize the summation of excitatory potentials, *Proc. Natl. Acad. Sci. USA*, Vol.103, pp.18799–18804 (2006).
13) Palmer, L.M. and Stuart, G.J.: Site of action potential initiation in layer 5 pyramidal neurons, *J. Neurosci.*, Vol.26, pp.1854–1863 (2006).
14) Gobel, W. and Helmchen, F.: New angles on neuronal dendrites *in vivo*, *J. Neurophysiol.*, Vol.98, pp.3770–3779 (2007).
15) Vucinic, D. and Sejnowski, T.J.: A compact multiphoton 3d imaging system for recording fast neuronal activity, *PLoS ONE*, Vol.2, e699, (2007).
16) Canepari, M., Djurisic, M., and Zecevic, D.: Dendritic signals from rat hippocampal CA1 pyramidal neurons during coincident pre- and post-synaptic activity: A combined voltage-and calcium-imaging study, *J. Physiol.*, Vol.580, pp.463–484, (2007).
17) Djurisic, M., Popovic, M., Carnevale, N., and Zecevic, D.: Functional structure of the mitral cell dendritic tuft in the rat olfactory bulb, *J. Neurosci.*, Vol.28, pp.4057–4068 (2008).
18) Geman, S. and Geman, D.: Stochastic relaxation, Gibbs distributions, and the Bayesian restoration of images, *IEEE Trans. Pattern. Anal. Mach. Intell.*, Vol.6 pp.721–741 (1984).
19) Tanaka, K.: Statistical-mechanical approach to image processing, *J. Phys. A*, Vol.35, R81–R150 (2002).
20) Rall, W.: Theory of physiological properties of dendrites, *Ann. N.Y. Acad. Sci.*, Vol.96, pp.1071–1092 (1962).
21) Rall, W.: Theoretical significance of dendritic trees for neuronal input-output relations, in *Neural Theory and Modeling*, ed. R.F. Reiss, Stanford University Press, pp.73–97 (1964).
22) Dempster, A.P., Laird, N.M. and Rubin, D.B.: Maximum Likelihood from Incomplete Data via the EM Algorithm, *J. Royal Statist. Soc. B*, Vol.39, No.1, pp.1–38 (1977).